

Supporting Information:

Observation of PH-Induced Protein Reorientation at the Water Surface

*Konrad Meister^{1,#}, Steven J. Roeters^{2,#}, Arja Paananen³, Sander Woutersen², Jan Versluis¹,
Géza R. Szilvay³ & Huib J. Bakker¹*

¹AMOLF, Science Park 104,

1098XG Amsterdam, The Netherlands

²Van 't Hoff Institute for Molecular Sciences, University of Amsterdam, Science Park 904,

1098 XH Amsterdam, The Netherlands

³VTT Technical Research Centre of Finland Ltd, PO. Box 1000, FI-02044 VTT, Espoo,

Finland

[#]These authors contributed equally to the presented work.

*Correspondence to: K.Meister@amolf.nl

The laser source for the VSFG setup is a regenerative Ti:Sapphire amplifier (Coherent) producing 800 nm pulses at a 1 kHz repetition rate with a pulse duration of 35 fs and a pulse energy of 3.5 mJ. Approximately one third of the laser output is used to pump a home-built optical parametric amplifier and a difference-frequency mixing stage. This nonlinear optical device produces tuneable broadband mid-IR pulses (ranging from 2-10 μm , 600 cm^{-1} bandwidth at FWHM, 10-20 μJ). The IR pulses have a sufficiently large bandwidth to measure the complete VSFG spectrum of the amide I vibrations. Another part of the 800 nm pulse is sent through an etalon to narrow down its bandwidth. The resulting narrow-band 800 nm pulse (VIS) and the broadband IR pulse are directed to the sample surface at angles of $\sim 47^\circ$ and $\sim 45^\circ$, respectively, to generate light at the sum frequency. The VIS and IR beams are focused in spatial and temporal overlap on the sample surface with 200 mm and 100 mm focal length lenses, respectively. The SFG light generated at the surface is sent to a monochromator and detected with an Electron-Multiplied Charge Coupled Device (EMCCD, Andor Technologies). Spectra are first background subtracted (blocked IR) and normalized to a reference SFG spectrum measured from z-cut quartz. As a measurement cell we used custom-made Teflon troughs. We performed measurements both in buffered systems (constant ionic strength) (100 mM phosphate buffer, 50 mM acetate buffer) and in pure $\text{H}_2\text{O}/\text{D}_2\text{O}$ and observed a similar pH-dependence for the buffered system as for pure water. The pH values was adjusted by adding sodium hydroxide or hydrochloric acid and samples were routinely checked (Mettler Toledo FE20) before and after each measurement. The pH values were changed either directly in the SFG trough, or by preparing HFBI solutions at different pH values. Both methods resulted in very similar spectral changes. The typical acquisition time of a VSFG spectrum was 600s. Class II hydrophobins HFBI and HFBII were provided by VTT research and purified as described elsewhere¹⁻².

We first determined the hydrophobic moment vector (HMV) of HFBI (PDB-ID: 2FZ6) by finding the average location of the hydrophilic and hydrophobic parts of the molecule and set the vector from the latter to the former³⁻⁴. We define ($\theta=0^\circ$, $\psi=0^\circ$, $\varphi=0^\circ$) so that the HMV is parallel to the surface normal (a position expected to be energetically favourable because most hydrophobic residues are outside the water, pointing into the air). We then perform spectral calculations as previously described⁵⁻⁷. In short, the VSFG response is calculated by constructing a 1-exciton Hamiltonian based on the crystal structure of the protein that is diagonalized to yield the IR and Raman response. By taking their tensor product the VSFG response is obtained. To estimate the coupling between nearest neighbours (dominated by through-bond effects) we use a parameterized map of an *ab initio* 6-31G+(d) B3LYP calculation⁸, while non-nearest neighbour coupling (dominated by through-space interactions) are estimated with the transition dipole coupling model⁹. An empirical model adapted from the literature¹⁰ is used to describe the influence of hydrogen bonds on the frequencies of the local amide-I modes. The VSFG spectra are then calculated by convoluting the obtained VSFG response with a Lorentzian to account for the homogeneous broadening. We found that the observed frequency splitting between the $\sim 1675\text{ cm}^{-1}$ and the $\sim 1635\text{ cm}^{-1}$ peak could best be reproduced by reducing the empirical parameters that correlate the hydrogen bond length to the resulting frequency shift by 20% with respect to the values used in reference 5. We derive the protein orientation by performing a global Levenberg-Marquardt fit of the resulting orientation-dependent VSFG response to the experimental SSP and PSP data from 1590-1710 cm^{-1} .

The presented fits consist of a global fit that includes both SSP and PSP data. The signal intensity of the SSP signal is much higher than the PSP signal, resulting in a much higher sensitivity of the fit parameters to the SSP spectrum than to the PSP spectrum. Performing a fit solely to the PSP data yields good agreement with the experimental data with parameters that are similar to those resulting from the global fit: $\theta = 32^\circ \pm 6^\circ$ and $\psi = 229^\circ \pm 10^\circ$ at high pH,

and $\theta = 40^\circ \pm 10^\circ$ and $\psi = 276^\circ \pm 10^\circ$ at low pH. For comparison, the global fit results in $\theta = 27^\circ \pm 3^\circ$ and $\psi = 214^\circ \pm 5^\circ$ at high pH, and $\theta = 44^\circ \pm 10^\circ$ and $\psi = 271^\circ \pm 10^\circ$ at low pH.

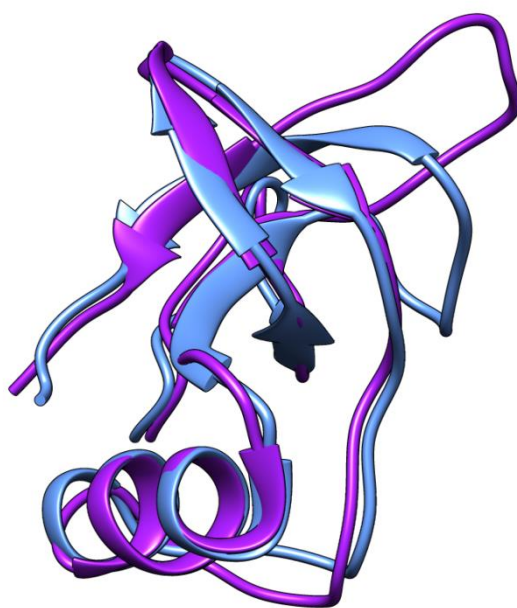
The uncertainties were determined by testing by how much θ or ψ must be changed so as to increase the residual sum of squares (RSS) by 100% after re-optimizing all other parameters (SFig. 7). We performed a grid search from $0 - 180^\circ$ for θ and $0 - 360^\circ$ for ψ with 10° intervals to make sure we did not end up in a local minimum. The RSS could be minimized by optimizing spectral parameters like the intrinsically unknown interfacial refractive index with respect to commonly used literature values without changing the interpretation: in all cases a small deviation from the hydrophobicity vector with respect to the surface normal is found for the high-pH spectra that increases when the pH is lowered.

The errors were estimated by fixing θ and ψ to varying values away from the global fit maxima and re-optimizing all other parameters (see SFig. 7). We find that the data is fitted best with a rather large homogeneous linewidth Γ (10 cm^{-1}). When using a smaller Γ of e.g. 6 cm^{-1} the angles obtained by fitting do not change much for the low-pH spectra ($\theta = 26.6^\circ$ and $\psi = 217.2^\circ$). For the high-pH fit the angles are $\theta = 58.3^\circ$ and $\psi = 282.1^\circ$ (while the RSS increases by 217% for the low-pH spectra and by 65% for the high-pH spectra. Hence, changing Γ does not influence the qualitative interpretation.

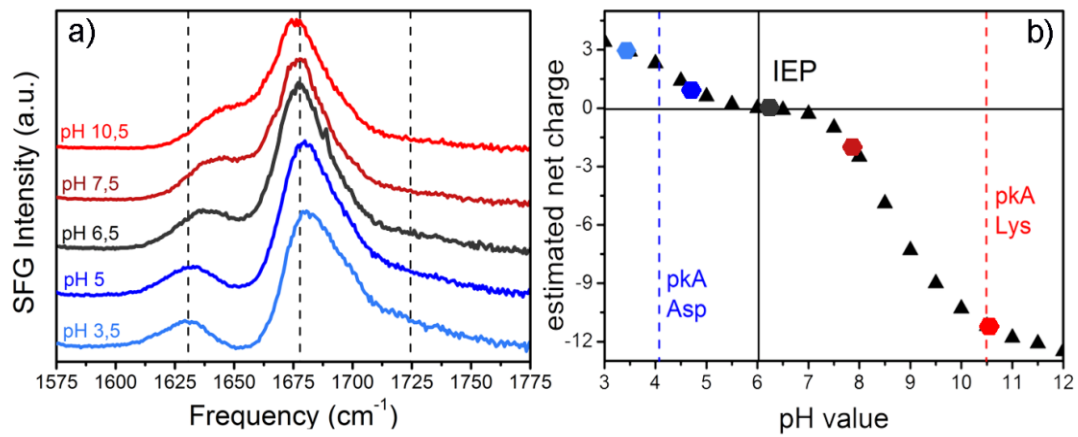
The same goes for fixing the interfacial refractive indices to a value found for layers of adsorbed proteins of $\sim 7.5 \text{ kDa}$ (the molecular weight of HFBI)¹¹: while the angles obtained by fitting them with the interfacial refractive index at both the sum frequency and at the visible frequency fixed to 1.5 did not change much with respect to the fit shown in the main text (in which the interfacial refractive indices were fitted), the RSS increased by 139% for the high-pH values and by 7% for the low-pH values. When both interfacial refractive indices were fixed to 1.5 the best fit resulted in $\theta=27.2^\circ$, $\psi = 217.3^\circ$ for the high-pH spectra, and $\theta = 44.9^\circ$ and $\psi = 271.7^\circ$ for the low-pH spectra.

In order to achieve this reduction in the RSS the interfacial refractive indices did not have to change more than 13% from the refractive index value found by Vörös *et al*¹¹. Changes of the interfacial refractive indices resulting from reorientations have been observed before. For example, for the liquid crystal 48-n-octyl-4-cyanobi-phenyl a change of 36% (from 1.4 to 1.9) upon an interfacial reorientation of 10° was observed¹²⁻¹³.

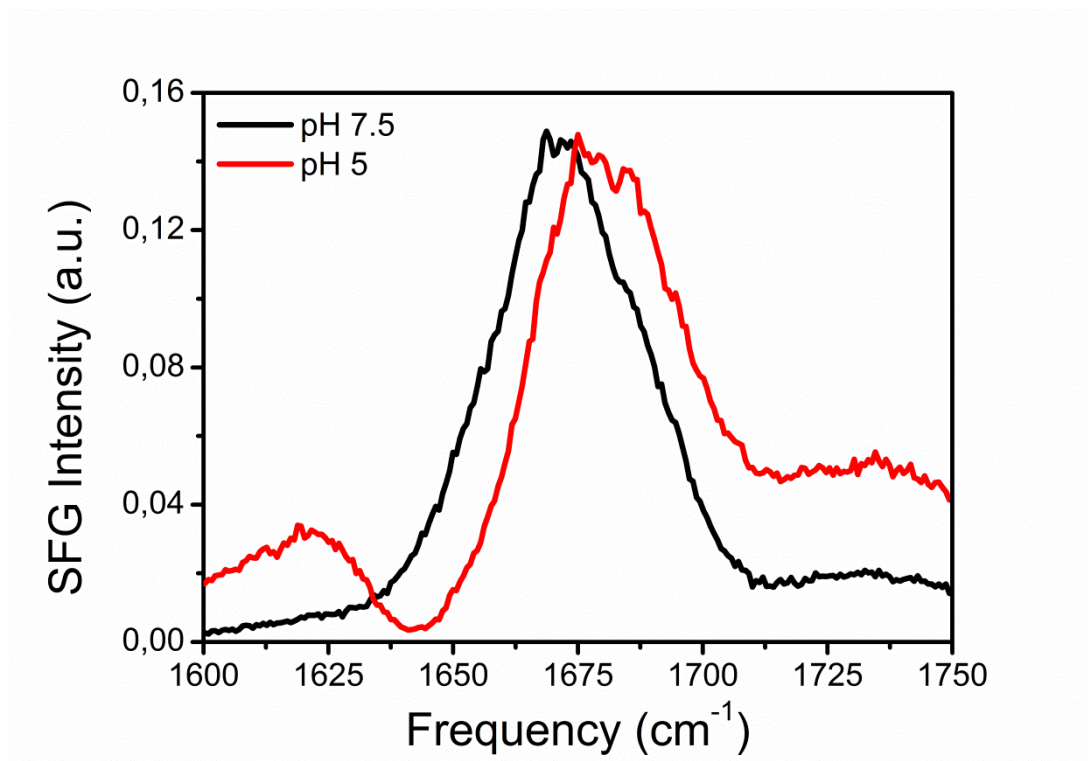
Finally, we studied the potential sensitivity of the calculation results with respect to a potential relative frequency shift of the SSP and PSP spectra, as it is difficult to exclude a relative shift of a few cm^{-1} in the experiment. We find the dependence of the fitted tilt angle on the relative spectral shift to be negligible, even for a very large relative shift of 15 cm^{-1} .



Supporting Figure 1: Structural superimposition of the crystal structures of the hydrophobins HFBI (blue) and HFBII (magenta). Both proteins are derived from the fungi *T. reesei* and share a similar fold that consist of a β -barrel core and a small α -helical part.

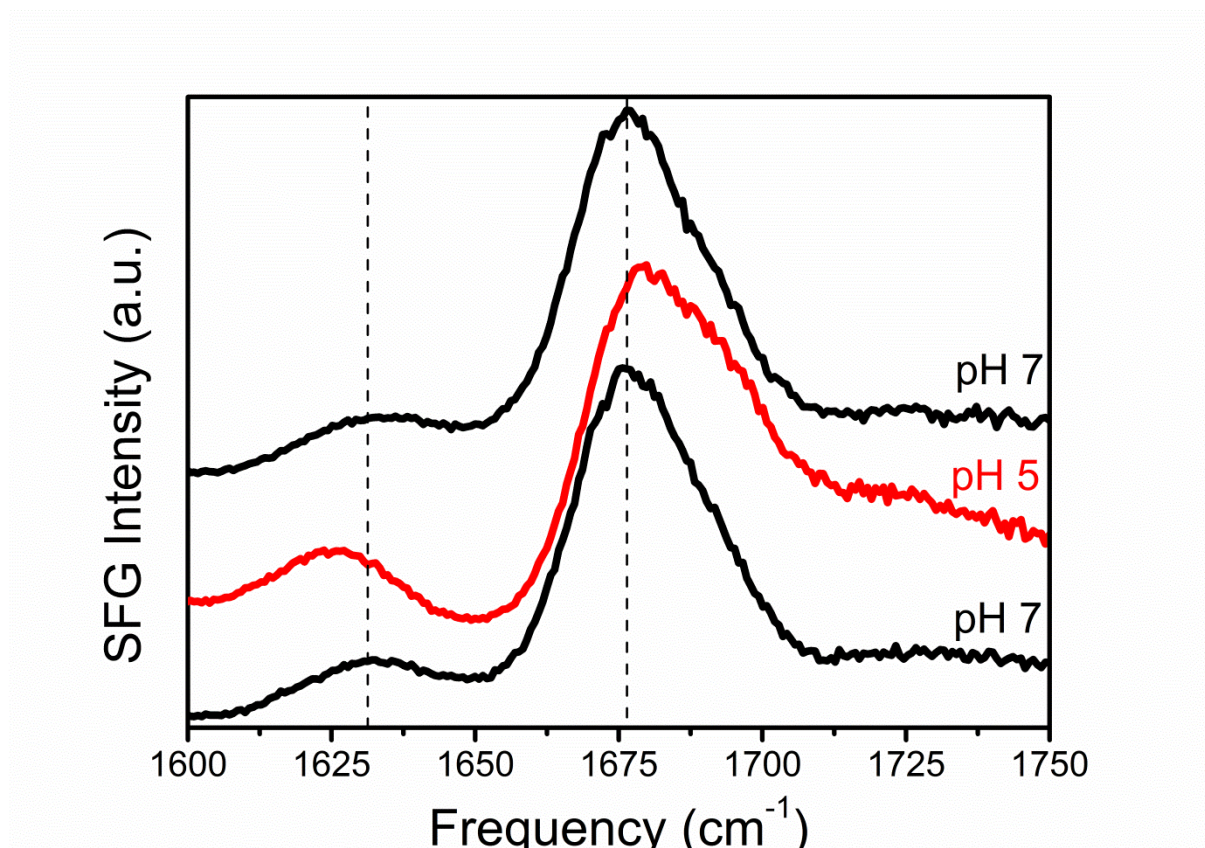


Supporting Figure 2: VSFG spectra of a 14 μM HFBI solution at different pH values and the corresponding estimated net charge state of the protein. (a) At acidic pH values (3-5) signals are observed at ~ 1630 , ~ 1680 and ~ 1725 cm^{-1} . Increasing the pH value towards the isoelectric point of HFBI (5-7) results in a red-shift of the band at 1680 cm^{-1} and a decrease of the amplitudes of the bands at 1725 cm^{-1} and 1630 cm^{-1} . (b) Calculated net charge of HFBI as a function of pH.

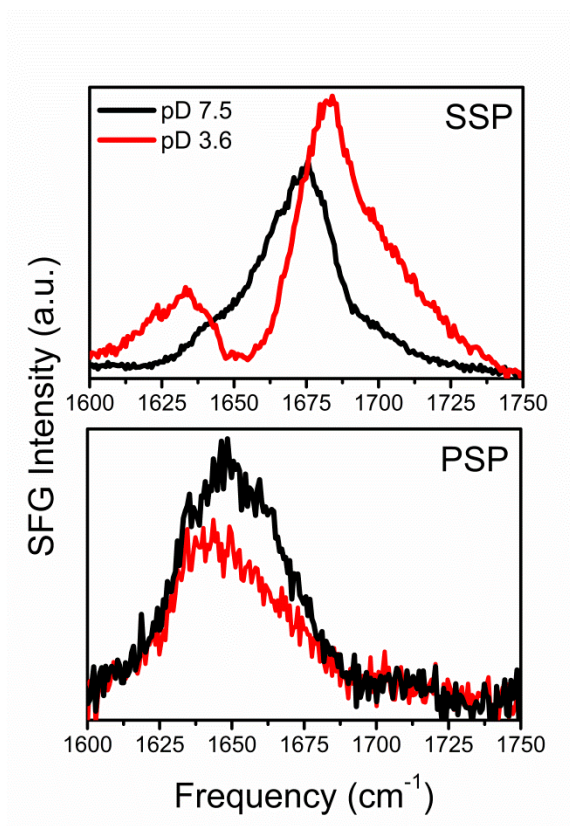


Supporting Figure 3: VSFG spectra of a 14 μM HFBII solution at two different pH values.

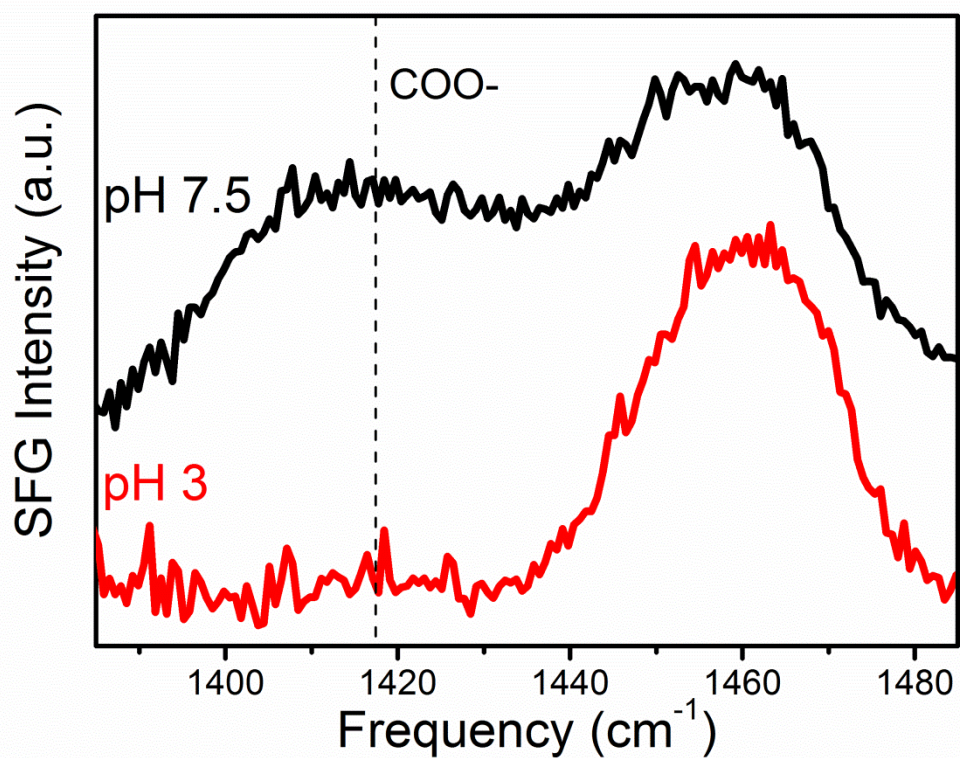
Changing the pH values leads to a similar shift as observed for HFBI.



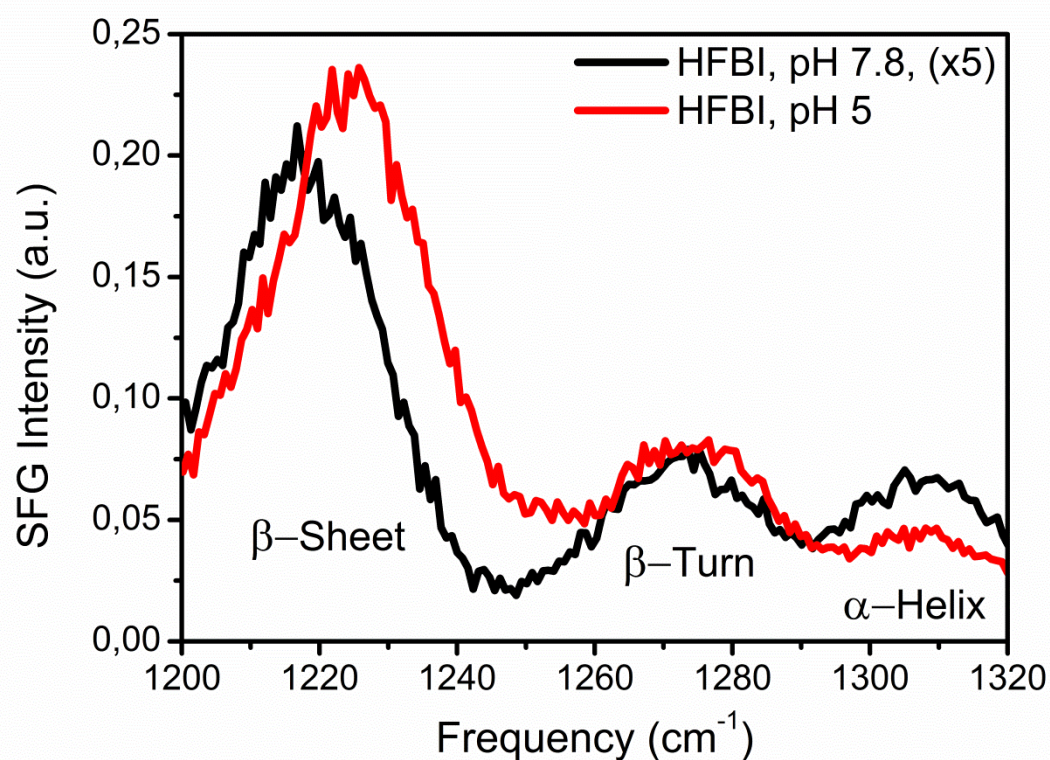
Supporting Figure 4: pH dependent VSFG spectra of a 14 μM HFBI solution at pH 7 (black, above) and pH 5 (red) and back at pH 7 (black, lower spectrum). The observed spectral changes are highly reversible.



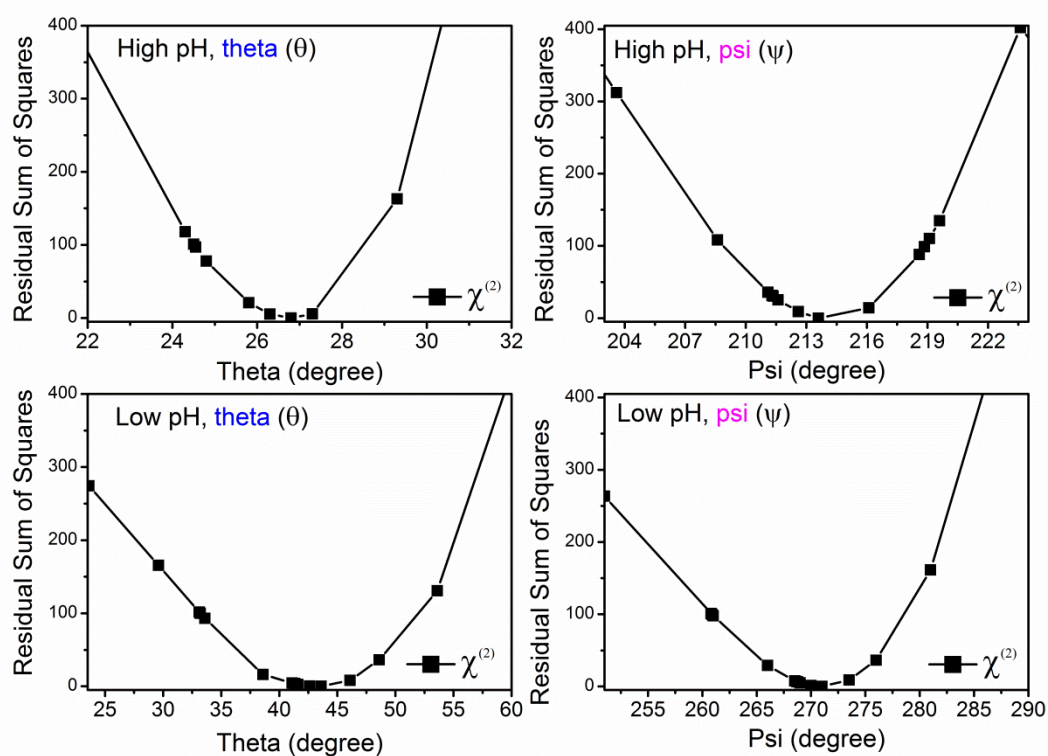
Supporting Figure 5: pD-dependent VSFG spectra of HFBI in deuterated water. Changing the pD values leads to a similar shift (1682 cm^{-1} to 1675 cm^{-1} ; $\sim 7\text{ cm}^{-1}$) of the amide I bands as in the achiral SSP spectra in water (1683 cm^{-1} to 1677 cm^{-1} ; $\sim 6\text{ cm}^{-1}$). Lowering the pH to an acidic value does not eliminate the PSP signal but changes the peak ratio of the 1640 cm^{-1} and 1660 cm^{-1} bands.



Supporting Figure 6: pH dependent VSFG spectra of HFBI in water. At acidic pH values the band at $\sim 1410\text{ cm}^{-1}$ vanishes due to protonation of the carboxyl group.



Supporting Figure 7: pH dependent VSFG spectra of a 14 uM HFBI solution at pH 5 (red, 50mM acetate buffer) and pH 7.8 (black, 100mM phosphate buffer). An increase in the intensity of the helical signal at 1305 cm^{-1} is observed at higher pH-values.



Supporting Figure 8: Dependency of the residual sum of squares of the fits on fixing theta (θ) and psi (ψ) away from the global fit minimum for pH = 8 (upper row) and pH = 4.5 (lower row).

References:

- (1) Paananen, A.; Vuorimaa, E.; Torkkeli, M.; Penttilä, M.; Kauranen, M.; Ikkala, O.; Lemmetyinen, H.; Serimaa, R.; Linder, M. B. Structural Hierarchy in Molecular Films of Two Class II Hydrophobins. *Biochemistry* **2003**, *42*, 5253-5258
- (2) Hakanpää, J.; Szilvay, G. R.; Kaljunen, H.; Maksimainen, M.; Linder, M.; Rouvinen, J., Two Crystal Structures of Trichoderma Reesei Hydrophobin HFBI -the Structure of a Protein Amphiphile with and without Detergent Interaction. *Protein Sci.* **2006**, *15*, 2129-2140
- (3) Reißer, S.; Strandberg, E.; Steinbrecher, T.; Ulrich, Anne S.; 3D Hydrophobic Moment Vectors as a Tool to Characterize the Surface Polarity of Amphiphilic Peptides. *Biophys. J* **2014**, *106*, 2385-2394.
- (4) <http://www.ibg.kit.edu/HM>
- (5) Roeters, S. J.; van Dijk, C. N.; Torres-Knoop, A.; Backus, E. H. G.; Campen, R. K.; Bonn, M.; Woutersen, S. Determining In Situ Protein Conformation and Orientation from the Amide-I Sum-Frequency Generation Spectrum: Theory and Experiment. *J. Phys. Chem. A.* **2013**, *117*, 6311-6322.
- (6) Schach, D.; Globisch, C.; Roeters, S. J.; Woutersen, S.; Fuchs, A.; Weiss, C. K.; Backus, E. H. G.; Landfester, K.; Bonn, M.; Peter, C.; Weidner, T. Sticky Water Surfaces: Helix–Coil Transitions Suppressed in a Cell-Penetrating Peptide at the Air-Water Interface. *J. Chem. Phys.* **2014**, *141*, 22D517.
- (7) Hennig, R.; Heidrich, J.; Saur, M.; Schmäser, L.; Roeters, S. J.; Hellmann, N.; Woutersen, S.; Bonn, M.; Weidner, T.; Markl, J.; Schneider, D. IM30 Triggers Membrane Fusion in Cyanobacteria and Chloroplasts. *Nature Comm.* **2015**, *6*, 7018.
- (8) Gorbunov, R. D.; Kosov, D. S.; Stock, G. Ab Initio-Based Exciton Model of Amide I Vibrations in Peptides: Definition, Conformational Dependence, and Transferability. *J. Chem. Phys.* **2005**, *122*, 224904.

- (9) Krimm, S.; Abe, Y.; Intermolecular Interaction Effects in the Amide I Vibrations of β -Polypeptides. *Proc. Natl. Acad. Sci. U.S.A.* **1972**, 69, 2788–2792
- (10) Hamm, P.; Zanni, M.; Concepts and Methods of 2D Infrared Spectroscopy. *Cambridge University Press*: Cambridge, **2011**
- (11) Vörös, J.; The Density and Refractive Index of Adsorbing Protein Layers. *Biophys. J.* **2004**, 87, 553-561
- (12) Ye, P.; Shen, Y. R.; Local-Field Effect on Linear and Nonlinear Optical Properties of Adsorbed Molecules, *Phys. Rev. B* **1983**, 28, 4288-4294
- (13) Wang, H.-F.; Gan, W.; Lu R.; Rao Y.; Wu, B.-H. Quantitative Spectral and Orientational Analysis in Surface Sum Frequency Generation Vibrational Spectroscopy (SFG-VS). *Int. Rev. Phys. Chem.* **2005**, 24, 191-256